2010

Quantifying Variance Due to Temporal and Spatial Difference Between Ship and Satellite Winds

Jackie Crystal May

THE FLORIDA STATE UNIVERSITY

COLLEGE OF ARTS AND SCIENCES

QUANTIFYING VARIANCE DUE TO TEMPORAL AND SPATIAL DIFFERENCE BETWEEN SHIP AND SATELLITE WINDS

By

JACKIE CRYSTAL MAY

A thesis submitted to the
Department of Earth, Ocean and Atmospheric Science
in partial fulfillment of the
requirements for the degree of
Master of Science

Degree Awarded:
Fall Semester, 2010

The members of the committee approve the thesis of Jackie C. May defended on October 25, 2010.

_____
Mark A. Bourassa
Professor Directing Thesis

_____
Vasubandhu Misra
Committee Member

_____
Zhaohua Wu
Committee Member

_____
Shawn R. Smith
Committee Member

The Graduate School has verified and approved the above-named committee members.

Dedicated to my husband, David May, for his endless love, support, and encouragement.

ACKNOWLEDGEMENTS

The funding for this research was provided through NOAA COD and NASA OVWST. I would like to thank my major professor, Dr. Mark Bourassa, for the opportunity to pursue my Master's degree. His continuous guidance and assistance has been greatly appreciated. I thank Dr. Vasubandhu Misra, Dr. Zhaohua Wu, and Shawn Smith for serving on my committee. An additional thanks goes to Shawn Smith for his assistance with any SAMOS-related question or problem that came up. I would also like to thank Paul Hughes for providing the flux lookup table. I thank Kathy Fearon for her guidance while I was writing my thesis. Finally, I would like to thank my family and friends, and especially my husband, for their continuous support.

TABLE OF CONTENTS

List of Tables vi
List of Figures vii
Abstract viii

1. INTRODUCTION 1

2. DATA 5

   2.1 Equivalent Neutral Winds 5
   2.2 SeaWinds Scatterometer 6
   2.3 SAMOS data 7
   2.4 Ocean Wave and Current Data 9

3. IDEALIZED SCENARIO 11

   3.1 Method 11
   3.2. Results 13

4. COLLOCATION AND COMPARISON METHOD 17

   4.1 SeaWinds and SAMOS collocations 17
   4.2 SeaWinds and SAMOS comparisons 20

5. RESULTS 23

6. SUMMARY 29

REFERENCES 31

BIOGRAPHICAL SKETCH 34

LIST OF TABLES

1 Recorded parameters by SAMOS with their respective units and accuracy. Metadata on the location and type of instrument are also available. 8

2 Vessels used in idealized case and comparison observations with SeaWinds 8

LIST OF FIGURES

1 Actual wind speed variance (solid black lines) and 10-meter EN wind speed variance (dashed red lines) as a function of (a) miscollocation in time and (b) miscollocation in time and wind speed. 15

2 Wind stress variance as a function of (a) miscollocation in time and (b) miscollocations in time and wind speed....16

3 Schematic showing an example of the SeaWinds and SAMOS collocation method using a single SAMOS observation and four SeaWinds wind vector cells. The time differences and the spatial differences are combined to find the total difference for each potential collocation. The minimum total difference is determined to be the closest collocation....19

4 Collocated SeaWinds-measured wind speeds versus adjusted SAMOS 10-meter equivalent wind speeds calculated by (a) neglecting the ocean surface term and (b) including the ocean surface term. Each of these collocations have wave and current data available, less than a 5 ms^{-1} wind speed difference, and less than a 45° difference in wind direction....23

5 Total variance calculated with the adjusted SAMOS 10-meter EN wind speed excluding the ocean surface term (black line) and including the ocean surface term (red line) for all of the collocated observations for each one-minute time difference, with a fifteen-minute running mean filter applied. 24

6 Total variance associated with the collocated observations, excluding the ocean surface term, within each wind speed group for each one-minute time difference, with a fifteen-minute running mean filter applied. 25

7 The idealized case temporal variance (red line) is added to the variance associated with the data sets for the 4-7 ms^{-1} wind speed group (blue line) to obtain the idealized case total variance (black line). 27

8 Total variance associated with the collocated observations, including the ocean surface term, within each wind speed group for each one-minute time difference, with a fifteen-minute running mean filter applied. 28

ABSTRACT

Ocean vector winds measured by the SeaWinds scatterometer onboard the QuikSCAT satellite can be validated with in situ data. Ideally the comparison in situ data would be collocated in both time and space to the satellite overpass; however, this is rarely the case because of the time sampling interval of the in situ data and the sparseness of data. To compensate for the lack of ideal collocations, in situ data that are within a certain time and space range of the satellite overpass are used for comparisons. To determine the total amount of random observational error, additional uncertainty from the temporal and spatial difference must be considered along with the uncertainty associated with the data sets. The purpose of this study is to quantify the amount of error associated with the two data sets, as well as the amount of error associated with the temporal and/or spatial difference between two observations.

The variance associated with a temporal difference between two observations is initially examined in an idealized case that includes only Shipboard Automated Meteorological and Oceanographic System (SAMOS) one-minute data. Temporal differences can be translated into spatial differences by using Taylor's hypothesis. The results show that as the time difference increases, the amount of variance increases. Higher wind speeds are also associated with a larger amount of variance. Collocated SeaWinds and SAMOS observations are used to determine the total variance associated with a temporal (equivalent) difference from 0 to 60 minutes. If the combined temporal and spatial difference is less than 25 minutes (equivalent), the variance associated with the temporal and spatial difference is offset by the observational errors, which are approximately 1.0 m^2s^{-2} for wind speeds between 4 and 7 ms^{-1} and approximately 1.5 m^2s^{-2} for wind speeds between 7 and 12 ms^{-1}. If the combined temporal and spatial difference is greater than 25 minutes (equivalent), then the variance associated with the temporal and spatial difference is no longer offset by the variance associated with observational error in the data sets; therefore, the total variance gradually increases as the time difference increases.

CHAPTER ONE

INTRODUCTION

Ocean surface wind vectors are important in many applications, including weather prediction, understanding dynamical forcing of the ocean, and studying air-sea interactions and climate [*Huddleston and Spencer*, 2001; *Liu*, 2002; *Bourassa et al*., 2010b]. Scatterometers, radar altimeters, synthetic aperture radars (SAR), microwave radiometers, and in situ observations provide different methods of obtaining wind speeds, and in some cases directions, globally over the ocean; however, scatterometers have proven to be the most effective instrument for retrieving ocean surface vector winds [*Liu and Xie*, 2006]. The primary purpose of spaceborne microwave scatterometers, such as the SeaWinds scatterometer onboard the QuikSCAT satellite, is to provide frequent global wind measurements over the ocean.

SeaWinds winds are often validated through comparison with in situ observations that are collocated in time and space to the satellite. Unfortunately, there is almost always some difference in time and/or space between the two observations. The first part of this study will quantify the amount of error that is associated with the temporal and/or spatial difference between two wind observations as a function of time and wind speed. These results will then be verified using collocated in situ and SeaWinds measurements. The amount of error associated with the temporal and spatial difference between SeaWinds and in situ-measured winds will be quantified, as well as the amount of error associated with the data sets.

Several studies [*Stoffelen*, 1998; *Freilich and Dunbar*, 1999; *Ebuchi et al*., 2002; *Bourassa et al*., 2003] have shown that collocated in situ observations can be used to calibrate and validate scatterometer wind vectors. Ideally, the in situ observations used for comparisons would be collocated in both time and space with the satellite overpass. In reality, however, these ideal collocations are rare. Two reasons for non-ideal collocations are that in situ data are sparse and the in situ sampling interval is large compared to the high along-track temporal sampling frequency of SeaWinds. Therefore, to compensate for the lack of ideally collocated comparison observations, observations that are within a certain time and space range of the satellite overpass are used for comparison. In a comparison of these two data sets, additional uncertainty due to the

temporal and/or spatial difference between the two observations should be considered along with the uncertainty associated with the in situ measurements and the scatterometer measurements.

Previous studies have examined the uncertainty due to spatial differences. *Kent et al*. [1999] used pairs of voluntary observing ship (VOS) observations with the same reporting hour to determine the random observational error variance for individual VOS meteorological variables, including 10-meter corrected wind speed. The study was limited to four months: January and July of 1980 and 1993. The mean wind speed variance was examined as a function of the spatial difference from 0 to 1000 km. The error variance in the wind speed was then calculated by extrapolating the variance between two observations to a zero amount of separation. The analysis determined the random observational error estimates for individual VOS parameters in 30° by 30° areas; the random error within these areas was found to range from 1.3 to 2.8 ms^{-1} for the 10-meter corrected wind speeds. Quality controlled observations from research vessels are usually more accurate [*Smith et al.,* 1999].

Different sources of uncertainty, including spatial difference, between SeaWinds and research vessel observations were identified and examined by *Bourassa et al*. [2003]. The wind vector uncertainty was examined as a function of the spatial difference between the research vessel and SeaWinds observations; however, the variance associated with a temporal difference was not considered. One of the limitations of the study was that only a few months of data were used for analysis; the more extensive data set used herein provides more robust results.

Unlike the previous studies, the study presented here determines the random observational variance as a function of both the spatial and temporal difference between two observations, instead of only the spatial difference. The spatial and temporal resolutions used to examine the variance in this study are much finer than those used by *Kent et al.* [1999]. This study will focus on temporal differences between observations of less than 30 minutes and spatial differences between observations of less than 30 km. Selecting a smaller range of acceptable temporal and spatial differences allows the total amount of variance associated with comparing two data sets to be examined as a function of the combined temporal and spatial difference. This method makes it possible for the variance associated with the temporal and spatial difference to be quantified independently from the variance associated with observational errors. Also, a much more extensive data set, including data from all months of the year for five years, is used in this analysis compared to either of the previously discussed studies.

The amount of uncertainty that can be attributed to a temporal and spatial difference between two wind observations is determined in this study by using an idealized case in which only in situ data are considered. In situ data are obtained from the Shipboard Automated Meteorological and Oceanographic System (SAMOS) initiative and consist of measurements collected at one-minute intervals over the period 2005–2009. For this idealized scenario, the satellite is assumed to pass directly over the ship every hour on the hour. Shifts of time from the assumed satellite overpass are used to examine the error associated with a mismatch in time. Taylor's hypothesis (frozen turbulence) [*Taylor*, 1938] can then be used to translate a temporal shift to a spatial shift. This uncertainty is also examined as a function of wind speed.

The second part of this study verifies the results from the first part using collocated SAMOS and SeaWinds observations. The total amount of random observational variance between the two observations is examined as a function of the spatial/temporal difference as well as a function of wind speed. The total variance can be separated into two components: the variance associated with a temporal and spatial difference between the two observations and the variance associated with the data sets. This separation allows for each of these variance components to be examined and quantified individually.

Knowing the variance associated with the temporal and spatial difference between two observations and the variance associated with the two data sets is useful in the calibration of other instruments, data assimilation, operational numerical weather prediction, development of geophysical model functions, and creation of gridded products [*Bourassa et al*., 2003; *Liu*, 2002]. The method presented in this analysis uses SeaWinds and SAMOS wind observations. Although SeaWinds recently ceased to function, it provided an extensive data set to work with and the results will be useful in reanalysis efforts. Also, the method presented in this analysis can be applied to any data set; it is not limited to only SeaWinds and SAMOS observations.

The conversion of in situ winds to equivalent neutral winds (the "winds" observed by satellite) is explained in Chapter 2. The data used in this conversion and for the comparison (SeaWinds, SAMOS, wave, and current data) are also described. The method used to determine the amount of variance as a function of space or time and wind speed in an idealized scenario is discussed in Chapter 3. In Chapter 4, the procedure for collocating the SeaWinds measurements, SAMOS observations, wave, and current data is described. Finally, the amount of uncertainty due to the temporal and spatial difference between the SeaWinds and SAMOS observations, as

well as the amount of uncertainty associated with the data sets, is determined as a function of time and wind speed. These results are presented in Chapter 5.

CHAPTER TWO

DATA

2.1 Equivalent Neutral Winds

Scatterometers operate by sending microwave pulses to the ocean surface and measuring the backscatter cross section from the surface roughness. The ocean surface is modified by surface capillary waves caused by wind stress [*Weissman et al*., 1994; *Bourassa et al*., 1999; *Liu and Xie,* 2006]. The wind stress is then calibrated into an "equivalent neutral" (EN) wind speed at a reference height of 10 meters [*Ross et al*., 1985; *Weissman et al*., 1994; *Portabella and Stoffelen*, 2009, *Bourassa et al*., 2010a]. The in situ comparison observations, used to validate the scatterometer measurements, must also be height adjusted to 10 meters and then converted from actual winds into EN winds. To adjust the actual wind speed measured at a given anemometer height to a reference height (z) of 10 meters, the following equation for the modified log-wind profile (equation 1) is used:

$$\boldsymbol{U}(z)-\boldsymbol{U}_{sfc}=\frac{\boldsymbol{u}_*}{\boldsymbol{\kappa}}\left[\ln\left(\frac{z}{z_0}+1\right)-\varphi(z,z_0,L)\right], \tag{1}$$

where the surface friction velocity ($\boldsymbol{u}_*$) is the square root of the kinematic stress ($\boldsymbol{\tau}/\rho$), $\boldsymbol{\tau}$ is the surface wind stress, ρ is the density of the air, z_o is the momentum roughness length, $\boldsymbol{U}$ is the wind speed at height z, $\boldsymbol{U}_{sfc}$ is the wind speed at the ocean surface, κ is the von Kármán's constant ($\kappa = 0.4$), φ is an atmospheric stability term, and L is the Monin-Obukhov scale length. Traditionally, EN winds differ from actual winds in that they assume neutral stratification in the atmosphere ($\varphi = 0$), but use the non-neutral values of u_* and z_o determined from equation (1) and a reference height of 10 meters. This approach was designed to allow the correct stress to be calculated from the equivalent neutral wind and a neutral drag coefficient.

Bourassa et al. [2010a] presented a revised definition of EN winds that includes a density adjustment term. The adjustment was necessary because an air density dependent error was found in the comparison of satellite and in situ equivalent neutral winds. This modification is

also consistent with the concept of a scatterometer responding (indirectly) to surface stress as opposed to the friction velocity. The revised definition for 10-meter EN wind (U_{10EN}) is:

$$\boldsymbol{U}_{10EN} - \boldsymbol{U}_{sfc} = \frac{\boldsymbol{u}_*}{\kappa}\left[\ln\left(\frac{z}{z_0}+1\right)\right]\sqrt{\frac{\rho}{\rho_0}}\,, \tag{2}$$

where ρ_0 is standard reference density of air set at 1.0 kg m^{-3}. A boundary layer model [*Bourassa*, 2006] based on the Bourassa, Vincent, and Wood (BVW) model [*Bourassa et al*., 1999] is used to adjust the in situ measured winds to U_{10EN} winds.

2.2 SeaWinds Scatterometer

The SeaWinds microwave scatterometer onboard the polar-orbiting QuikSCAT satellite was launched into space on 19 June 1999. Initially, its mission was to continue scatterometer coverage after the payload malfunction of the Advanced Earth Observing Satellite (ADEOS-I), until ADEOS-II could be launched. Unfortunately, ADEOS-II was operational for only six months. QuikSCAT, on the other hand, remained operational until late 2009. It provided over 10 years of continuous global coverage and has proven to be beneficial to both operational and research efforts.

SeaWinds operated in the microwave band at 13.4 GHz using two rotating pencil-beam antennas. The inner beam was horizontally polarized with an incidence angle of 46.25° and a radius of 707 km, whereas the outer beam was vertically polarized with an incidence angle of 54° and a radius of 900 km. By operating in the microwave band, SeaWinds was able to sample the Earth's surface in both clear and cloudy conditions throughout the day and night. There were between 8 and 20 radar cross sections (footprints) that were combined into 25-by-25-km wind cells. The center of each wind cell was the center of mass of all of the footprints within that cell. Up to 76 wind cells composed the 1800-km-wide observation swath, with the most accurate observations found between 200 and 700 km from nadir [*Bourassa et al*., 2003]. Subsequent reprocessing resulted in the regions of higher quality data being extended much closer to nadir.

The SeaWinds version 3 swath data produced by the Remote Sensing Systems, reprocessed to add updated radiometer data to the files, are used in this study. The Ku-2001

geophysical model function was used to retrieve the wind data. . The SeaWinds wind data and additional details are available online from the Remote Sensing Systems (http://www.remss.com).

One of the limitations of scatterometers, is that rain can have adverse effects on the scatterometer wind retrieval process. Rain can alter the radar signal through scattering and two-way attenuation. Also, sea surface roughness is changed by the impact of the raindrops [*Weissman et al*., 2002; *Bourassa et al*., 2003; *Draper and Long*, 2004]. The SeaWinds data set obtained from the Remote Sensing Systems contains several rain flags that are used to identify seriously rain contaminated scatterometer data, and data for which there are insufficient radiometer observations to provide a radiometer-based flag. As suggested by Remote Sensing Systems, data identified with the following flags have been omitted from this study: expected quality of the vector retrieval (iclass) = 0 (no retrieval), scatterometer rain flag (irain_scat) = 1 (indicates rain), radiometer rain rate (rad_rain) > 0.15, and time difference between scatterometer and collocated radiometer (min_diff) > 30.

2.3 SAMOS Data

Two of the most commonly used types of in situ data for scatterometer comparisons are buoy data and research vessel data. Compared to winds measured by research vessels, buoy winds are more intermittent (albeit more plentiful in space) and modifications caused by the sea state are more problematic [*Bourassa et al*., 2003]. Therefore, in situ data used in this study are composed of the data collected through the Shipboard Automated Meteorological and Oceanographic Systems (SAMOS) initiative that serves to archive research vessel observations.

The SAMOS initiative is complementary to the Voluntary Observing Ship (VOS) project, which collects and reports in situ data every one to six hours. A SAMOS automatically records navigational, meteorological, and oceanographic parameters with a computerized data logging system at one-minute intervals [*Smith et al*., 2010]. The instruments on research vessels tend to be better sited and maintained than instruments on typical VOS platforms. Although the VOS project has much denser spatial coverage because it includes more vessels, SAMOS has a much higher temporal sampling, which is more advantageous to some research topics. The SAMOS initiative became operational as of 2005, and the data are available online from the Research

Vessel Surface Meteorology Data Center (http://samos.coaps.fsu.edu/html/data_availability.php). The recorded parameters are given in Table 1, along with their respective units and accuracy [*Bradley and Fairall*, 2006].

Table 1: Recorded parameters by SAMOS with their respective units and accuracy. Metadata on the location and type of instrument are also available.

Variable	Units	Accuracy of Mean
Ship position	Latitude, longitude (degrees)	0.001°
Ship course over ground	Degrees (clockwise from true north)	2°
Ship speed over ground	Knots	Larger of 2% or 0.2 ms^{-1} (0.4 knots)
Ship heading	Degrees (clockwise from true north)	2°
Ship-relative wind speed	Meter per second	Larger of 2% or 0.2 ms^{-1} (0.4 knots)
Ship-relative wind direction	Degrees (clockwise from bow)	3°
Earth-relative (true) wind speed	Meter per second	Larger of 2% or 0.2 ms^{-1} (0.4 knots)
Earth-relative (true) wind direction	Degrees (clockwise from true north)	3°
Air temperature	Degrees Celsius	0.2°C
Atmospheric pressure	Millibar	0.1 mb
Relative humidity	Percent	2%
Precipitation	Millimeter	~ 0.4 mm/day
Radiation	Watts per $meter^2$	5 W/m^2
Sea temperature	Degrees Celsius	0.1°C

Eight SAMOS-equipped research vessels are used in this study. The research vessel name, location of cruise track, and dates of available data are given in Table 2. The spatial range of these ships includes the Atlantic, Pacific, Gulf of Alaska, Southern Ocean, and Arctic Ocean. All seasons of the year in both hemispheres have been sampled. Since many different geophysical conditions are sampled in this study, there is unlikely to be a bias due to a particular location or time of year.

Table 2: Vessels used in idealized case and comparison observations with SeaWinds.

Research Vessel	Location	Available data
Atlantis	North Atlantic and North	June 2005 – November 2009
David Star Jordan	North Pacific	March 2008 – April 2009
Healy	Gulf of Alaska and Arctic	June 2007 – October 2009
Henry B. Bigelow	North Atlantic	April 2007 – November 2009
Knorr	Atlantic and Pacific	May 2005 – November 2009
Laurence M. Gould	Southern Ocean	April 2007 – November 2009
Miller Freeman	Gulf of Alaska	January 2007 – October 2009
Southern Surveyor	South Pacific	April 2008 – November 2009

The version 200 SAMOS data, which have undergone common formatting, metadata enhancement, and automated quality control [*Smith et al*., 2010], are used in this study. Version 200 data have been compacted into daily files and are available from 2005 onward. Although this data set has not undergone visual inspection or further quality control it is the most complete SAMOS data set currently available. To make the SAMOS-recorded winds comparable to SeaWinds observations, the winds are adjusted to U_{10EN} using the method discussed in section 2.1.

2.4 Ocean and Current Data

Scatterometers respond to the ocean surface roughness, which is modified by the wind stress. Surface stress is primarily dependent on the wind shear [*Bourassa*, 2004]. Therefore, scatterometer-measured wind speeds are more closely related to the wind shear than they are to the equivalent neutral wind speed at 10 meters. By including the horizontal motion of the ocean surface due to ocean waves and currents with the SAMOS-determined 10-meter EN wind speeds, more accurate surface-relative in situ comparison data can be obtained. Model wave and current data are used in this study to represent the ocean surface. The model outputs are bilinearly interpolated to the location of the research vessel winds.

The ocean wave data used in this study were obtained from the global National Oceanic and Atmospheric Administration (NOAA) WAVEWATCH III (NWW3) ocean wave model. The spatial coverage of this model is from 77° S to 77° N, with a 1.25° longitudinal and 1.0° latitudinal grid spacing. The temporal resolution is every three hours. Output from this model includes zonal and meridional wind speed, significant wave height, peak wave period, and peak wave direction. Additional details about the model are available online from NOAA (http://polar.ncep.noaa.gov/waves/implementations.shtml).

The ocean current data used in this study were obtained from the Ocean Surface Current Analyses – Real Time (OSCAR) global data set from NOAA. OSCAR data provide operational ocean surface velocity, or currents, from satellite fields [*Bonjean and Lagerloef*, 2002]. Both the zonal and meridional ocean surface currents are given on a global 1.0° by 1.0° grid spacing at approximately five-day intervals. The spatial coverage of this product is from 69.5° S to 69.5° N.

Further details of this project can be found online at the NOAA Web site (http://www.oscar.noaa.gov).

CHAPTER THREE

IDEALIZED SCENARIO

3.1 Method

This idealized study is designed to examine the natural variability associated with a temporal difference between two observations. Only the temporal difference will be considered here; there is assumed to be no spatial difference. Three parameters will be examined in this idealized scenario: actual wind speed (U_{10}), 10-meter EN wind speed (U_{10EN}), and wind stress. The variance of these parameters will be determined as both a function of the temporal difference as well as a function of wind speed.

In this idealized case only in situ data are considered: the one-minute observations collected through the SAMOS initiative from 2005 through 2009. A pseudosatellite is assumed to pass directly over the ship every hour on the hour; therefore, every hourly SAMOS observation is considered an ideal collocation in both time and space to the pseudosatellite overpass. To match the sampling of SAMOS to a satellite, a time-averaging window is defined using Taylor's hypothesis [*Taylor*, 1938], or frozen turbulence. Frozen turbulence means that characteristics of the turbulence are "frozen" in time. Taylor's hypothesis allows for a spatial dimension to be converted to a temporal dimension, and vice versa. To easily understand this concept, one can apply it to the driving difference between two cities. For example, the interstate driving distance between Tallahassee, Florida, and Mobile, Alabama, is approximately 250 miles. If someone drives 70 miles per hour on the interstate, then it would take that person roughly 3.5 hours (distance/speed) to drive that distance. Therefore, the driving difference between the two cities can be expressed as either a spatial difference or temporal difference.

Taylor's hypothesis, or frozen turbulence, is used to define a time-averaging window (t_{win}) centered on the hourly observation, equation 3. For a given volume of air (*footprint*) and speed at which it is traveling ($\overline{U}$), it is possible to determine how long (t_{win}) it would take to sample the total given volume.

$$t_{win} = \frac{footprint}{\left|\overline{U}\right|} \ , \tag{3}$$

where *footprint* is the SeaWinds footprint size (*footprint* = 7 km) and $\overline{U}$ is the average wind speed within the time-averaging window. As discussed in section 2.2, SeaWinds footprints were binned into 25-by-25-km cells; however, it has been shown that scatterometer sampling characteristics are better matched to winds on much smaller spatial scales [*Long*, 2002; *Bourassa et al*., 2003]. *Bourassa et al*. [2003] determined the balance between signal and noise in the research vessel observations best matches the scatterometer winds at a spatial-temporal scale of approximately 5 km. A spatial scale of 7 km was determined as the best match by David Long (personal communication, 2003). The study presented here, like the study by *Bourassa et al*. [2003], contains research vessel and scatterometer observations; therefore, a footprint size of 7 km, instead of 25 km, is used for the remainder of the study.

The size of the time-averaging window varies based on the average wind speed within that time-averaging window. Low wind speeds correspond with large time-averaging windows, and high wind speeds correspond with small time-averaging windows. The average wind speed within each window, however, cannot be determined unless the size of the time-averaging window is known. Therefore, an iterative process is used starting with a first guess of five minutes for the time-averaging window. The average wind speed within this time-averaging window is then calculated to obtain a new time-averaging window. This process is repeated until a steady solution, when the initial time-averaging window and the new time-averaging window are within 1.5 minutes of each other, is obtained. If a stable solution is not found, that hourly observation is omitted from the idealized case data set. The new time-averaging window is then assumed to be the time-averaging window centered on the hourly observation, thus representing an ideal collocation. Because wind speed varies with time, a fixed time-averaging window cannot be used for every hour. Therefore, this iterative process is replicated for each hour in the SAMOS data set.

To represent comparison data that are not ideally collocated in time to the pseudosatellite, the center of the hourly time-averaging window is shifted away from the hourly observation in one-minute increments. The size of the time-averaging window remains the same as it is shifted. For each one-minute shift, new average values are determined within the shifted time-averaging

window. The variance (σ_j^2) of all of the observations with a j-minute time shift is calculated from the difference between the hourly averages ($\overline{\boldsymbol{U}}_{i,j=0}$) and the time-shifted averages ($\overline{\boldsymbol{U}}_{i,j}$) for each one-minute shift using equation 4:

$$\sigma_j^2 = \frac{1}{N_j - 1} \sum_{i=1}^{N_i} \left(\left| \overline{\boldsymbol{U}}_{i,j} - \overline{\boldsymbol{U}}_{i,j=0} \right| \right)^2 , \tag{4}$$

where N is the number of observations with a j-minute time shift.

The variance is calculated for time differences from 0 to 60 minutes for three parameters: earth-relative wind speed, wind stress, and EN wind speed at 10 meters. Since SAMOS records actual wind speed, the average wind speed within each time-averaging window can be calculated easily. As discussed in Chapter 2, all of the one-minute SAMOS wind speed observations are translated into EN wind speeds at 10 meters using the BVW model; therefore, the average EN wind speed within each time-averaging window also can be obtained easily. Part of the translation from the anemometer recorded wind speed to EN wind speed includes calculating the surface wind stress using the observed atmospheric stability. As a result, the wind stress for each one-minute observation is known, which allows for the average wind stress within each time-averaging window to be calculated also.

In addition to determining the variance as a function of the time difference, it is also possible to examine the variance as a function of wind speed. The wind speed is grouped into intervals of 4 ms^{-1}. For example, in the first group, the wind speed ranges from 0 to 4 ms^{-1}, in the second group, the wind speed would range from 4 to 8 ms^{-1}, and so on. For each wind speed group, the variance of the differences is calculated for time differences from 0 to 60 minutes using equation 4 for each of the examined parameters. This method allows for examination of wind speed dependence of this variance.

3.2 Results

The variance of both U_{10} and U_{10EN} is examined as a function of the time difference from 0 to 60 minutes (Figure 1a) as well as a function of wind speed (Figure 1b). The variance of each of these parameters follows the same trends. The total amount of variance begins at zero with a

zero-minute time difference, which would represent a perfect collocation and would therefore not have any miscollocation variance associated with it. The total amount of variance increases as the time difference between two observations increases (looking horizontally). Figure 1b also shows that the larger the wind speed, the greater the associated variance (looking vertically). The increasing trend in the variance is due to the fact that wind speed changes rapidly with time. The larger the time difference is between two observations, the greater the difference in wind speed would be. The larger the wind speed difference is, the larger the variance of the difference in wind speed would be. The highest wind speed group (>12 ms^{-1}) is seen to have a more significant increase in the variance than the other three wind speed groups have. This increase is a result of the wind speed distribution within this wind speed group; there is a much broader range of wind speeds sampled in this group compared to the other 4 ms^{-1} groups.

Figure 1a shows that the total variance associated with U_{10EN} is slightly greater than the total variance associated with U_{10}. This characteristic can be explained by the typically unstable atmosphere found over the ocean: the ocean surface temperature is commonly warmer than the air temperature above. For unstable atmospheric conditions, EN winds, which are a better comparison to wind stress than actual winds, are stronger than actual winds [*Kara et al*., 2008], and the variability in wind increases as the wind speed increases. Changes in wind speed in unstable conditions are associated with two resulting processes that partially compensate for each other. An increased wind speed results in more wind shear and hence more stress. However, the increased wind speed also causes more mechanical mixing, which leads to a more stable atmosphere; a more stable atmosphere is associated with less wind stress [*Kara et al*., 2008]. These effects can be seen in Figure 1b with the different wind speed groups. For low to moderate wind speeds, changes in U_{10EN} are compensated for by the associated changes in atmospheric stability; therefore, the variability associated with U_{10EN} is approximately equal to that of U_{10} in the two lowest wind speed groups. For larger wind speeds, the atmospheric stability has less influence and cannot compensate for the greater variability associated with the larger wind speeds. Therefore, the variability associated with U_{10EN} is greater than that of U_{10} in the higher wind speed groups.

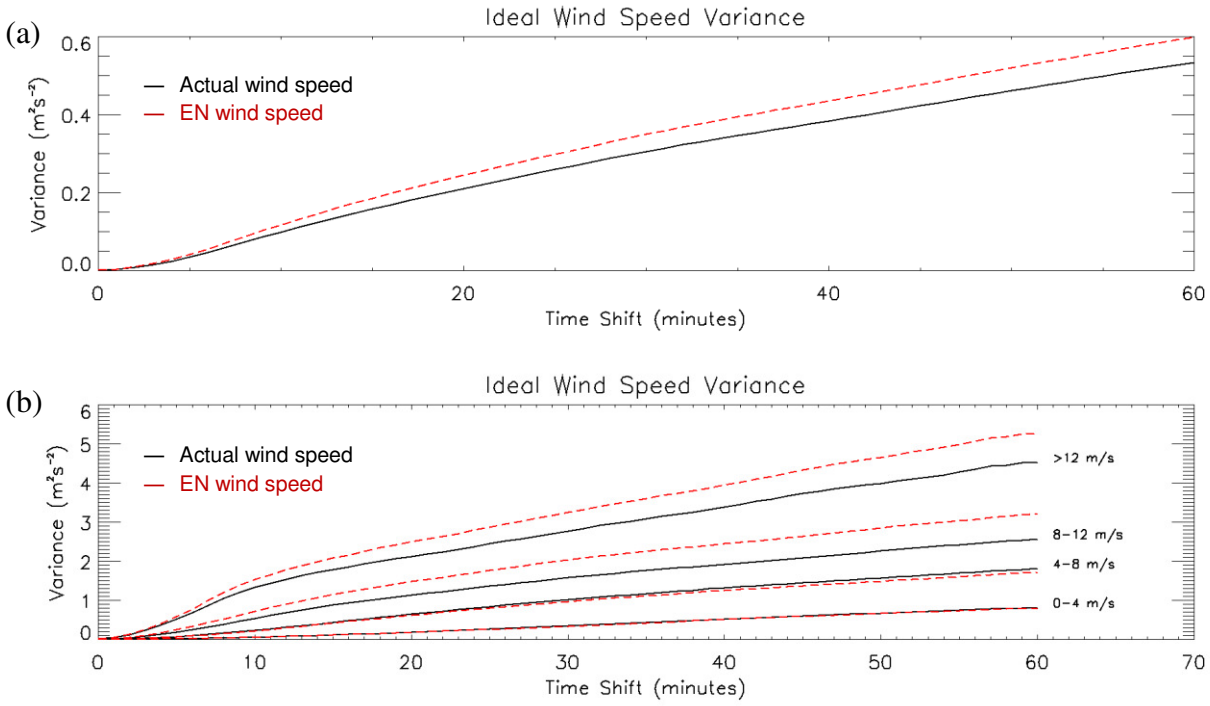

Figure 1. Actual wind speed variance (solid black lines) and 10-meter EN wind speed variance (dashed red lines) as a function of (a) miscollocation in time and (b) miscollocation in time and wind speed.

The variance associated with the wind stress is also examined in this idealized case, as shown in Figure 2. At this time there is no comparison to scatterometer wind stress values; however, there are plans to calibrate scatterometers to wind stress. Therefore, the variance of wind stress is shown here for completeness. The trends of the wind stress variance are similar to those found in the variance of both U_{10} and $U_{10\mathrm{EN}}$. As time increases, the amount of variance in the wind stress increases (Figure 2a). The amount of variance also increases as the wind speed increases (Figure 2b), with a more substantial increase in the highest wind speed group. Because surface stress is primarily dependent on wind shear, there is a non-linear dependency on wind speed. Wind stress ($\boldsymbol{\tau}$) does not increase linearly with the equivalent neutral wind speeds:

$$\boldsymbol{\tau} = \rho C_D U_{10EN} \left| \boldsymbol{U}_{10EN} \right|, \tag{5}$$

where ρ is the air density and C_D is the neutral drag coefficient.

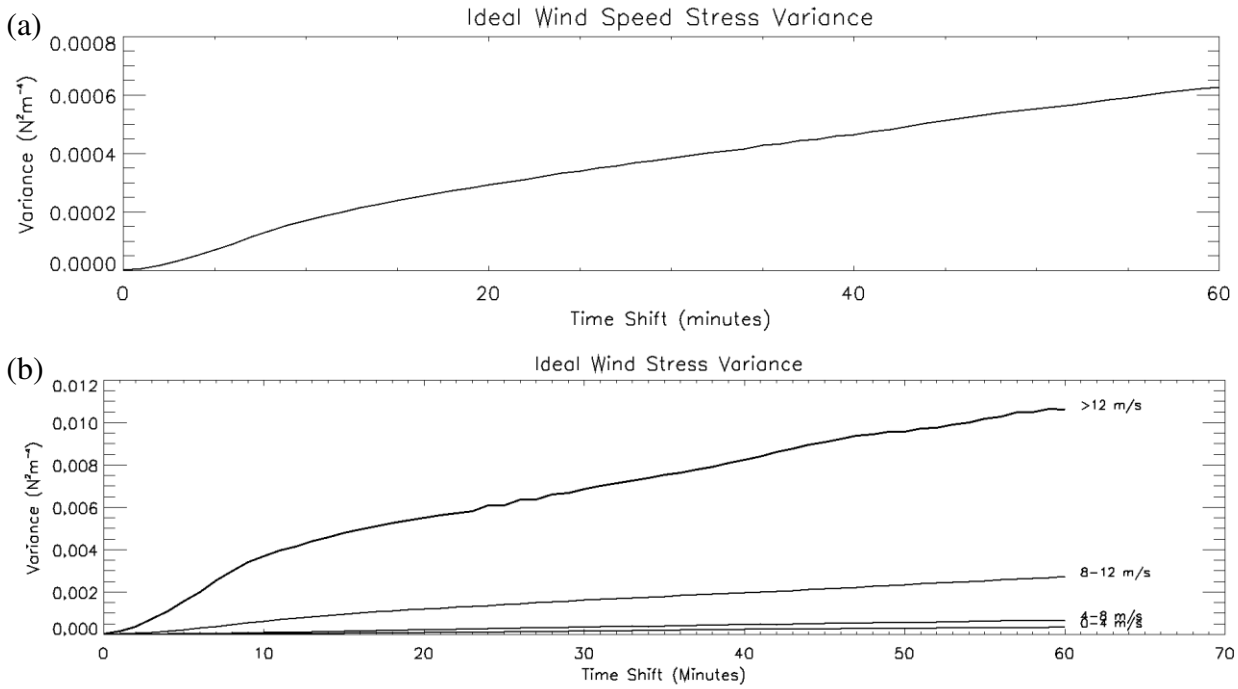

Figure 2. Wind stress variance as a function of (a) miscollocation in time and (b) miscollocation in time and wind speed.

CHAPTER FOUR

COLLOCATION AND COMPARISON METHOD

4.1 SeaWinds and SAMOS Collocations

The idealized case results are verified using collocated SeaWinds and SAMOS observations. Because the SeaWinds scatterometer is onboard a polar-orbiting satellite, any given surface location will be sampled on the order of once per day. Therefore, it is reasonable to assume that daily collocated SeaWinds and SAMOS observations can be obtained. Using the collocated observations, the variance due to the temporal and spatial difference between the two observations and the variance due to the data sets can be determined.

As discussed in section 2.2, SeaWinds has up to 76 wind vector cells composing the 1800-km-wide observation swath. As SeaWinds passes over a SAMOS vessel, multiple SeaWinds wind vector cells are in close proximity to the one-minute SAMOS observations. Because the closest collocation in both time and space is desired for this study, all of the SeaWinds wind vector cells and all of the SAMOS observations that are within 30 minutes and 30 km of each other are examined. To find the closest collocation, the combined temporal and spatial difference needs to be determined for each of the observations within the predefined range. Although, a temporal difference between two observations is not the same as a spatial difference between two observations, it is possible to combine the two differences by using Taylor's hypothesis, or frozen turbulence. This method, as discussed in section 3.1, allows for a spatial difference (*space_diff*) to be translated into a temporal difference (*converted_space*). It is also possible to translate a temporal difference into a spatial difference using this same method. However, since the variance in the idealized case was examined as a function of time, the difference in the SeaWinds and SAMOS observations are examined as a function of time as well for consistency. This translation is accomplished by using equation 6:

$$converted\_space = \frac{space\_diff}{|U_{sat}|}, \tag{6}$$

where U_{sat} is the SeaWinds-measured wind speed.

Because the spatial difference and the temporal difference are independent of each other, the combined total difference in minutes (*total_diff*) can be calculated from the root mean square (rms) sum of the converted spatial difference and the temporal difference (*time_diff*). Equation 7 shows this calculation:

$$total\_diff = \sqrt{time\_diff^2 + converted\_space^2} \tag{7}$$

The total difference is calculated for each of the SeaWinds wind vector cells and SAMOS observations within the predefined 30-minute and 30-km range. The SeaWinds wind vector cell and the SAMOS observation corresponding to the minimum total difference is considered to be the closest collocation.

An extremely exaggerated example of the collocation procedure can be seen in Figure 3. Only one SAMOS observation and four SeaWinds wind vector cells are used in this example to determine the closest collocation. The time differences between the SAMOS observation and each of the SeaWinds wind vector cells can be determined by using the reporting times given by the observations. Likewise, the spatial differences between the SAMOS observation and the center of each of the SeaWinds wind vector cells can also be determined by using the given latitudes and longitudes corresponding to the observations. For this example, an assumed constant SeaWinds wind speed of 10 ms^{-1} is used to convert the spatial differences into temporal differences using Taylor's hypothesis (i.e., for cell 4 the converted space is equal to $9000\text{m}/(10\text{m s}^{-1}\ 60\text{s min}^{-1})$, which equals 15 minutes). The converted spatial difference can then be added to the temporal difference to find a total combined difference as an rms sum (i.e., for cell 4 the total difference is equal to $\sqrt{(5\text{min}^2 + 15\text{min}^2)}$, which equals 15.81 minutes). This process is repeated for each of the SeaWinds wind vector cells. The minimum total difference can then be determined (i.e., the SeaWinds wind vector cell with the arrow) and is considered to be the closest collocation in both time and space.

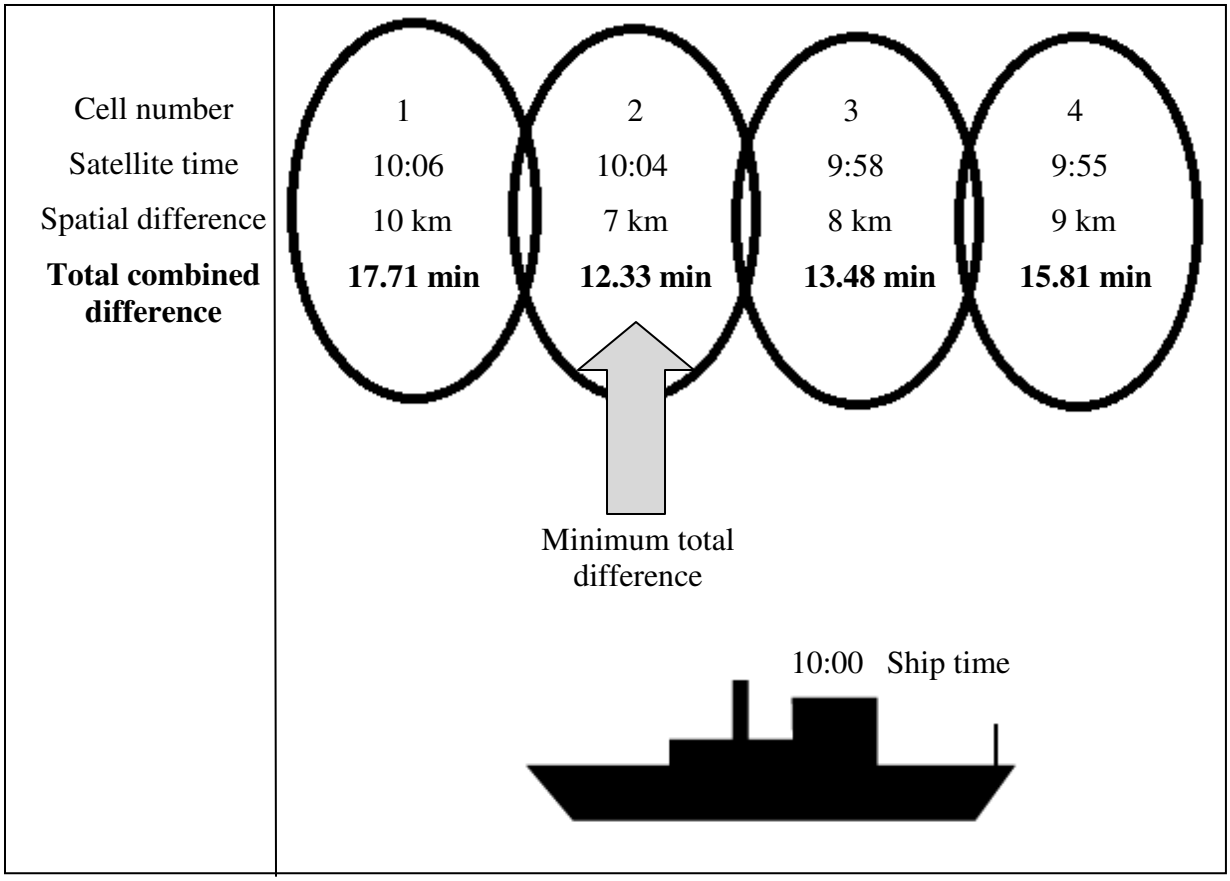

Figure 3. Schematic showing an example of the SeaWinds and SAMOS collocation method using a single SAMOS observation and four SeaWinds wind vector cells. The time differences and the spatial differences are combined to find the total difference for each potential collocation. The minimum total difference is determined to be the closest collocation.

Spatial differences and temporal differences each have an impact on the total difference. As seen in the simplified example in Figure 3, the spatial difference has a larger impact than the temporal difference. The schematic above shows that the closest collocation corresponds to the smallest spatial difference (cell 2), not the smallest temporal difference (cell 3). The relative importance is a function of the actual differences and the wind speed. The spatial difference converted into a temporal difference will often have a higher equivalent temporal difference compared to the original temporal difference; therefore, the spatial difference would have a more significant impact than the temporal difference in most cases.

Because the SAMOS data are provided every minute, a time-averaging window (t_{win}) for the SAMOS data needs to be defined to ensure the sampling from SAMOS matches the sampling from SeaWinds:

$$t_{win} = \frac{footprint}{|U_{sat}|}, \tag{8}$$

where *footprint* is the footprint size of SeaWinds (*footprint* = 7 km) and U_{sat} is the satellite wind speed for the given collocation. The average SAMOS 10-meter EN wind speed is calculated within the time-averaging window for comparison to the collocated SeaWinds observation. This process of finding the closest collocation and then finding the SAMOS time-averaging window is done for every SeaWinds overpass.

4.2 SeaWinds and SAMOS Comparisons

After the closest collocation and the associated time-averaging window are determined, the collocated SeaWinds and SAMOS observations can be compared. Although the actual U_{10}, U_{10EN}, and wind stress are examined in the idealized case, only the EN wind speed can be compared in the real world since SeaWinds currently provides only U_{10EN}. As discussed in section 2.2, scatterometers respond to the wind stress. Therefore, the U_{10EN} provided by SeaWinds is a measure of the wind stress (shear), as opposed to the wind speed at 10 meters. Consequently, considering the horizontal motion of the ocean surface in the calculation of the SAMOS U_{10EN} would theoretically provide better comparison data to SeaWinds observations. To determine if including the ocean surface does or does not improve the comparison between SeaWinds- and SAMOS-measured winds, two average SAMOS 10-meter, equivalent neutral wind speeds, one without the ocean surface term (U_{10EN}) and one with them (U_{10EN}*), are calculated using equation (2) from section 2.1 within each of the time-averaging windows for comparison to the collocated SeaWinds observation.

The U_{10EN} is determined by setting the ocean surface term ($\boldsymbol{U}_{sfc}$) equal to zero. U_{10EN} * includes the horizontal motion of the ocean surface due to ocean waves and currents. The waves and currents data are obtained from model data and are then bilinearly interpolated to the location of the ship. The $\boldsymbol{U}_{sfc}$ term is computed using:

$$\boldsymbol{U}_{sfc} = \boldsymbol{U}_{curr} + 0.8\boldsymbol{U}_{orb}, \tag{9}$$

where $\boldsymbol{U}_{curr}$ is the surface current and $\boldsymbol{U}_{orb}$ is the orbital velocity. By including the $\boldsymbol{U}_{sfc}$ term in computing U_{10EN}*, the wind shear is being accounted for.

Wave data are used to estimate how waves influence the wind shear by modifying the lower boundary condition on velocity. The orbital velocity term ($\boldsymbol{U}_{orb}$) is used to transform the velocity frame of reference to a fraction of the orbital velocity of the dominant waves [*Bourassa*, 2004]. The orbital velocity is a function of the significant wave height (H_s) and the corresponding significant wave height period (T_p):

$$\boldsymbol{U}_{orb} = \frac{\pi H_s}{T_p} \tag{10}$$

The fraction of the orbital velocity that modifies the surface wind is 80% [*Bourassa*, 2006] and should be removed from the vector wind.

When SeaWinds is compared to U_{10EN}*, there are fewer collocated observations because there are areas where the wave and current data are not available. The waves and currents models output values over the ocean, not over land. Therefore, if the closest collocation corresponds to the SAMOS vessel being close to the coastline, then there will be no model data available. Only the collocated observations that have waves and currents available are examined.

Additional collocations are removed from the collocated data set because the differences are far too large to be due to random errors: the collocated data are likely on different sides of an atmospheric front, the SAMOS data are in error, or the scatterometer wind could be seriously rain impacted but not properly flagged. As discussed in section 2.3, the SAMOS data that are used in this study have not been visually quality controlled. Spikes in wind speed that would be determined as flawed by a visual inspection could pass the automated quality control and therefore be present in this data set. The difference between the collocated SeaWinds and SAMOS U_{10EN} measurements should be well within 5 ms^{-1} and the difference between the collocated wind directions should be no more than 45° for correctly selected ambiguities. Because of the design and wind retrieval process of scatterometers, a unique wind direction must be selected from one or more likely solutions. This process is called ambiguity selection. For wind speeds less than 3 ms^{-1}, SeaWinds is known to have some ambiguity selection error

[*Bourassa et al*., 2003]. The wind direction constraint eliminates collocated observations for which ambiguity errors are associated with large errors in direction. There are viewing geometries in which much smaller ambiguity directions can be expected: these smaller errors are not removed from the comparison data set.

Once the acceptable collocations have been determined, U_{10EN} and U_{10EN} * can be compared with SeaWinds. For each of the collocations, the total difference in minutes between the SeaWinds and SAMOS observations is determined (equation 7). The total variance (σ_j^2) of the difference between the SeaWinds-measured wind speed and the SAMOS average 10-meter EN wind speed ($\Delta \boldsymbol{U}_{i,j}$) is calculated using all of the collocations with a j-minute total time difference in equation 11:

$$\sigma_j^2 = \frac{1}{N_j - 1} \sum_{i=1}^{N_j} \left(\Delta \boldsymbol{U}_{i,j} \right)^2 , \tag{11}$$

where N is the number of observations with a j-minute time shift. The total variance is calculated for both comparison data sets as a function of the total difference to determine the effect of including or not including the ocean surface. Each of the total variances is also examined as a function of wind speed to determine the variance associated with the data sets versus the variance associated with the temporal and spatial difference between the observations.

CHAPTER FIVE

RESULTS

Figure 4 shows scatterplots of the collocated SeaWinds-measured wind speeds compared to U_{10EN} (Figure 4a) and compared to U_{10EN}* (Figure 4b) that meet the constraints identified in Chapter 4. When the ocean surface term is included in the calculation for the 10-meter EN wind speed, the best fit line between the two data sets is closer to a one-to-one correlation. These results suggest that including the ocean surface term provides a better 10-meter EN wind speed for comparison.

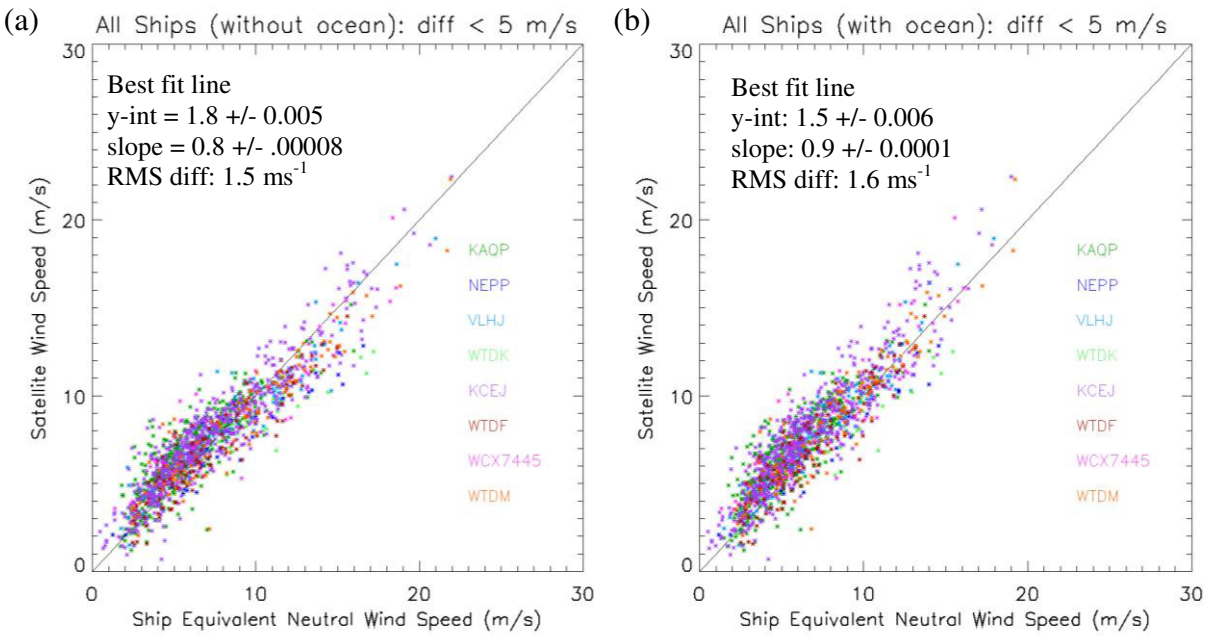

Figure 4. Collocated SeaWinds-measured wind speeds versus adjusted SAMOS 10-meter equivalent wind speeds calculated by (a) neglecting the ocean surface term and (b) including the ocean surface term. Each of these collocations have wave and current data available, less than a 5 ms^{-1} wind speed difference, and less than a 45° difference in wind direction.

For each data set, the total variance associated with all collocations with a j-minute temporal (equivalent) difference is examined. Unfortunately, calculating only the variance associated with each of these temporal bins produces extremely noisy results. The excessive noise makes it difficult to extract any discernible information about the variance. Therefore, a

15-minute running mean, or box-car filter, is applied to smooth the total variance. Figure 5 shows the smoothed total variance for each data set. One notable feature in this figure is that the total variance calculated from U_{10EN}* is slightly less than the total variance calculated from U_{10EN}. U_{10EN} considers the atmospheric contribution to shear, but ignores the ocean's motion. However, by including the ocean surface term in U_{10EN}*, the shear within that layer is more appropriately represented for calculating stress (see section 4.2). The lower total variance when surface motion is considered supports the idea that scatterometers respond more to wind shear than to earth-relative air motion [*Kelly et al*. 2001; *Cornillion and Park*, 2001; *Chelton et al*. 2004].

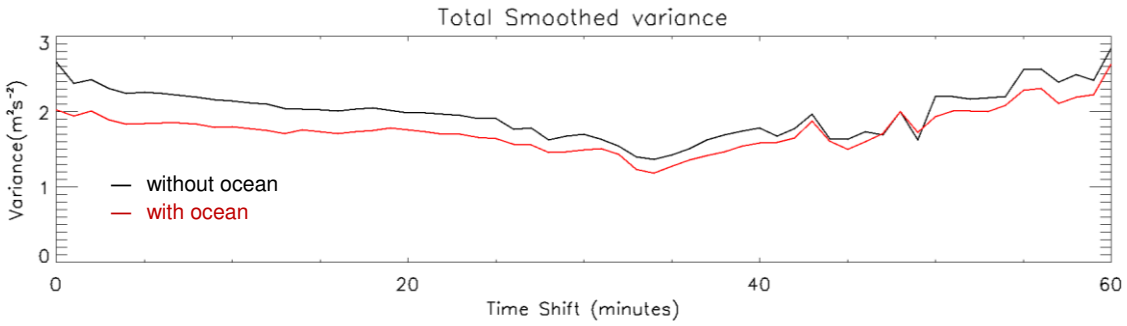

Figure 5. Total variance calculated with the adjusted SAMOS 10-meter EN wind speed excluding the ocean surface term (black line) and including the ocean surface term (red line) for all of the collocated observations for each one-minute time difference, with a fifteen-minute running mean filter applied.

The other notable feature in Figure 5 is the trend in the total variance. Initially, the total variance decreases as the time difference increases. After approximately a 30-minute time difference, the total variance begins to increase as the time difference increases. On the basis of the idealized case results, a general increasing trend should be seen for all time differences. Therefore, to determine the cause of the initial decreasing trend found in the collocated results, the total variance is separated into three different wind speed groups: 0-4 ms^{-1}, 4-7 ms^{-1}, and 7-12 ms^{-1}. Instead of calculating the variance of all of the collocations for each one-minute time difference, the variance of the collocations within a certain wind speed range for each one-minute time difference is calculated.

The total variance, separated into the three wind speed groups, is shown for U_{10EN} (Figure 6). If there are fewer than ten collocations within a given one-minute time difference, the sample

size is considered to be too small and the total variance associated with that time difference is not calculated. The lowest wind speed group, 0-4 ms^{-1}, appears to be the wind speed group that is not consistent with the idealized case results. There are several factors that could influence the results in this wind speed group. The first consideration is that scatterometers have greater difficulty accurately measuring wind speeds less than 3 ms^{-1} primarily because of ambiguity selection errors [*Bourassa et al.*, 2003]. Another problem with this lowest wind speed group is that it is associated with the largest time-averaging window when Taylor's hypothesis is applied. For example, a 3 ms^{-1} wind speed corresponds to a time-averaging window of 39 minutes; in comparison, a 6 ms^{-1} wind speed corresponds to a 19-minute time-averaging window. It is assumed that the statistics of the wind speeds remain the same within the time-averaging window; however, this is not a reasonable assumption for large time-averaging windows because wind speed changes rapidly with time. Conversely, for very high wind speeds, the time averaging window determined using Taylor's hypothesis is too short to have sufficient sampling when sampled in one minute intervals. All wind speeds examined in this study correspond to an adequately large time averaging window; therefore, the threshold when the wind speed becomes too high cannot be determined in this analysis. The problems associated with the lowest wind speed group make it difficult to determine any significant meaning in the total variance for that speed range. Therefore, only the total variance associated with wind speeds greater than or equal to 4 ms^{-1} are further examined.

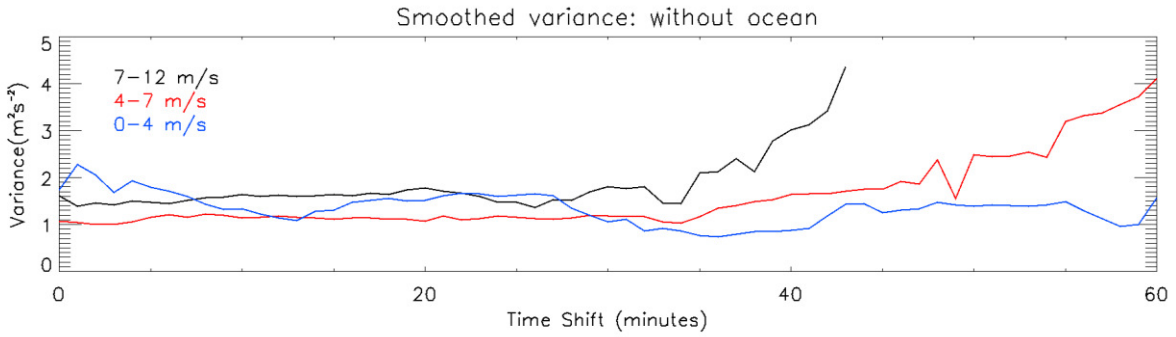

Figure 6. Total variance associated with the collocated observations, excluding the ocean surface term, within each wind speed group for each one-minute time difference, with a fifteen-minute running mean filter applied.

The curves seen in Figure 6 represent the total variance, which is composed of the variance in the data sets as well as the variance associated with the temporal and spatial difference between the two observations. The variance associated with the data sets should be relatively constant, whereas the variance associated with the temporal and spatial difference should gradually increase as the time difference increases, as shown in the idealized case. The relatively constant total variance that is seen from a 0- to 25-minute time (equivalent) difference shows the time differences for which the variance associated with observational errors in the data sets dominates the variance associated with the temporal and spatial differences between the two observations. The total variance found in this region is representative of the total observational error variance associated with the two collocated data sets: SeaWinds and SAMOS. Therefore; it can be deduced, from Figure 6, that this total variance between well-collocated SeaWinds and SAMOS observations for $7 < U_{10} < 12$ ms^{-1} is approximately 1.5 m^{2}s^{-2}, which corresponds to an approximate standard deviation of 1.2 ms^{-1}. For $4 < U_{10} < 7$ ms^{-1}, the total variance associated with the two data sets is approximately 1.0 m^{2}s^{-2}.

After a 25-minute time (equivalent) difference, the total variance in Figure 6 gradually increases as the time-equivalent difference increases. This gradual increase in total variance occurs because the variance associated with the temporal and spatial difference between the two observations is no longer offset by the variance associated with the two collocated data sets. In other words, the variance associated with the data sets is no longer the dominating term in the total variance. Therefore, after a 25-minute time (equivalent) difference, the variance associated with the temporal and spatial difference between two observations begins to have an impact on the total observed variance. Also of note in Figure 6 is that the total variance associated with the 7-12 ms^{-1} wind speed group is greater than the total variance associated with the 4-7 ms^{-1} wind speed group. As in the idealized case, larger wind speeds correspond to larger total variances.

If the variance associated with the data sets was added to the idealized case temporal variance found in section 3.2, then theoretically, the resulting total variance would look similar to that shown in Figure 6. The idealized total variance, along with the individual variance components, is shown in Figure 7 (black line) for the idealized 4-7 ms^{-1} wind speed group. Figure 7 shows a relatively constant total variance until approximately a 10-minute time difference, followed by a gradual increase in the total variance. This increase occurs at a smaller time difference compared to the increase seen at 25 minutes in Figure 6. Although the idealized

case and the real world are not expected to be exactly the same, this much difference between the two was not anticipated. Therefore, further investigation is required.

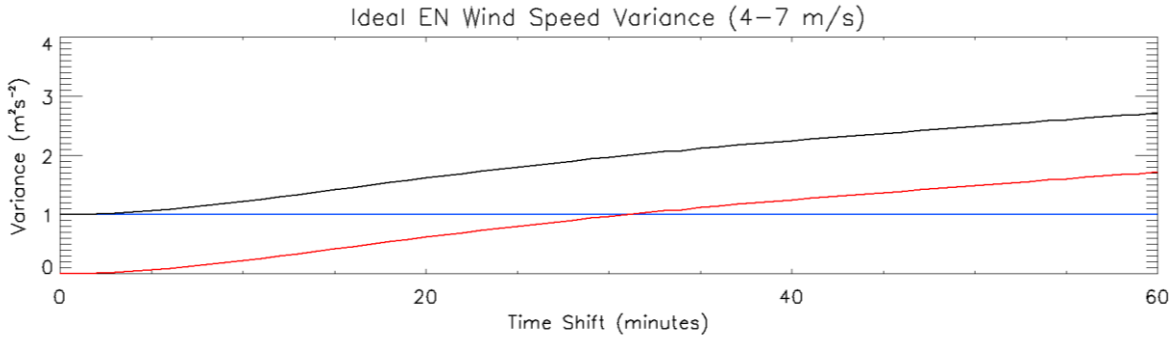

Figure 7. The idealized case temporal variance (red line) is added to the variance associated with the data sets for the 4-7 ms^{-1} wind speed group (blue line) to obtain the idealized case total variance (black line).

Examining the different elements within each wind speed group in the real world in more detail reveals an unexpected trend in the wind speed distributions as the time difference increases. For small time differences, all wind speeds within the predefined wind speed range are uniformly represented. However, as the time difference increases, the amount of wind speeds at the lower end of the predefined wind speed range increases while the amount of wind speeds at the upper end of the predefined wind speed range decreases. As discussed and shown before, lower wind speeds are associated with a lower amount of variance. Therefore, this change in wind speed distribution with increasing time shift results in a reduced variance with increasing time. For effective time differences less than roughly 25 minutes (and speed bin widths of 3 or 4 ms^{-1}), the decrease due to the changing wind speed distribution approximately compensates for the increased variance due to increasing time differences. The variance associated with the data sets remains the dominating term for an extended period of time differences, until roughly 25 minutes, in the real world. It is expected that if the wind speed groups defined in the real world were smaller (every 1 ms^{-1}), then the resulting total variance would be much closer to that seen in the idealized case total variance (Figure 7). Unfortunately, this study does not have enough data for smaller wind speed bins to be represented adequately; about three times the amount of data would be required.

The total variance separated into wind speed groups is shown U_{10EN}* in Figure 8. Once again, the total variance is not calculated for time differences containing fewer than 10 collocations. Because of the problems previously discussed respective to the lowest wind speed group, 0-4 ms^{-1}, only the variance associated with the 4-7 ms^{-1} and 7-12 ms^{-1} wind speed groups are shown in Figure 8. Qualitatively, the total variance associated with the U_{10EN}* is similar to the total variance associated with U_{10EN}. A relatively constant total variance is seen initially until roughly a 25-minute time (equivalent) difference because of the variance associated with the data sets dominating the variance associated with the temporal and spatial difference between the observations. The gradual increase in the total variance after about a 25-minute time (equivalent) difference is seen because the variance associated with the temporal and spatial difference between observations is no longer offset by the variance associated with the data sets. Also, the larger wind speed group has a higher total variance associated with it.

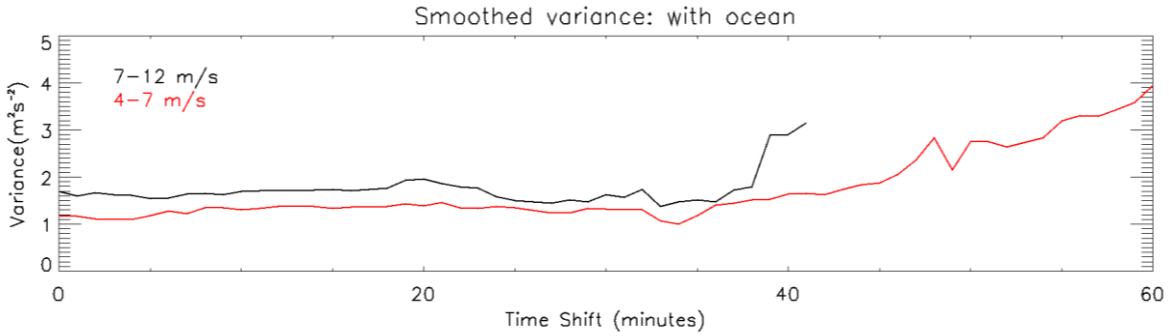

Figure 8. Total variance associated with the collocated observations, including the ocean surface term, within each wind speed group for each one-minute time difference, with a fifteen-minute running mean filter applied.

CHAPTER SIX

SUMMARY

The variance associated with the temporal and spatial difference between two well-collocated ship and satellite wind observations, as well as the variance associated with observational errors in these data sets, is determined. The satellite data were obtained from the SeaWinds scatterometer onboard the QuikSCAT satellite. The ship wind speed data were obtained from the Shipboard Automated Meteorological and Oceanographic System (SAMOS) initiative and then converted into 10-meter Equivalent Neutral (EN) wind speeds using a modified log-wind profile.

The variance associated with a temporal difference between two observations is first examined in an idealized case using only SAMOS data. This variance of the difference between two observations is examined for actual wind speeds (U_{10}), 10-meter EN wind speeds (U_{10EN}), and stresses. The analysis shows that the total variance associated with U_{10EN} is slightly less than the variance associated with U_{10} for low to moderate winds speeds, but larger for greater wind speeds. For unstable conditions, $U_{10\mathrm{EN}}$ is greater than U_{10}, and the variability in wind increases with increasing wind speed. For low to moderate winds speeds, changes in $U_{10\mathrm{EN}}$ due to atmospheric stability offset changes in wind speeds. For larger wind speeds, however, the changes due to stability are reduced and cannot compensate for the greater variability associated with larger wind speeds. The idealized case shows that for both the actual wind speed and EN wind speed, as the time difference between two observations increases, the amount of variance increases. Also, higher wind speeds are found to be associated with a larger amount of variance.

The results from the idealized case are verified using collocated SeaWinds and SAMOS data. The changes associated with considering the motion of the ocean surface ($U_{10\mathrm{EN}}$*) are examined in the comparison of SAMOS-measured wind speeds to 10-meter EN wind speeds ($U_{10\mathrm{EN}}$). Modeled waves and currents data are used to represent the ocean surface. The total variances of the data set that includes the ocean surface data and the data set that does not include these data are compared. The data set using the ocean surface data is found to be a better comparison to SeaWinds. The total variance associated with the collocations is also examined as a function of the temporal and spatial difference between the observations as well as a function

of wind speed. As in the idealized case, the higher wind speeds are found to correspond to a larger total variance. A relatively constant total variance of approximately 1.5 m^2s^{-2} for $7 < U_{10} < 12$ ms^{-1} and 1.0 m^2s^{-2} for $4 < U_{10} < 7$ ms^{-1} is found until roughly a 25-minute (equivalent) time difference. This initial constant variance represents the time differences for which the variance associated with observational error in the data sets is the dominant term in the total variance. After a 25-minute (equivalent) time difference, the variance gradually increases as the time difference increases, as seen in the idealized case. This increasing total observational variance is due to the variance associated with the spatial and temporal difference between the observations; the variance associated with observational errors is no longer the dominating term and therefore the total variance is no longer constant. It can then be deduced that if collocated ship and satellite observations have greater than a 25-minute (equivalent) difference, the variance associated with the temporal and spatial difference needs to be accounted for in the total variance; however, for collocations with less than a 25-minute (equivalent) difference, the variance associated with only the data sets needs to be considered for the total variance.

REFERENCES

Bonjean F. and G.S.E. Lagerloef (2002), Diagnostic model and analysis of the surface currents in the tropical Pacific ocean, *J. Phys. Oceanogr*., 32, 2,938-2,954.

Bourassa, M. A. (2004), An improved sea state dependency for surface stress derived from in situ and remotely sensed winds. *Advances in Space Res*., 33, 1136-1142.

—, M. A. (2006), Satellite-based observations of surface turbulent stress during severe weather, *Atmosphere - ocean interactions, Vol 2.*, W. Perrie, 35-52.

—, M. A., D. G. Vincent, W. L. Wood (1999), A flux parameterization including the effects of capillary waves and sea state, *J. Atmos. Sci.,*56, 1123-1139.

—, M. A., D. M. Legler, J. J. O'Brien, and S. R. Smith (2003), SeaWinds validation with research vessels, *J. Geophys. Res.,* 108, doi:10.1029/2001JC001081.

—, M. A., E. Rodriguez, R. Gaston (2010a), NASA's Ocean Vector Winds Science Team Workshops, *Bull. Amer. Meteor. Soc.*, 91, 925–928. doi: 10.1175/2010BAMS2880.1.

—, M. A., H. Bonekamp, P. Chang, D. Chelton, J. Courtney, R. Edson, J. Figa, Y. He, H. Hersbach, K. Hilburn, T. Lee, W. T. Liu, D. Long, K. Kelly, R. Knabb, E. Lindstorm, W. Perrie, M. Portabella, M. Powell, E. Rodriguez, D. Smith, A. Stoffelen, V. Swail, F. Wentz (2010b), Remotely sensed winds and wind stresses for marine forecasting and ocean modeling. Proceedings of the OceanObs'09: Sustained Ocean Observations and Information for Society Conference (Vol. 2), Venice, Italy, eds. J. Hall, D.E. Harrison and D. Stammer, ESA Publication WPP-306. (in press).

Bradley, F. and C. Fairall (2006), A guide to making climate quality meteorological and flux measurements at sea, *NOAA Tech. Memo.*, OAR PSD-311.

Chelton D. B., M. G. Schlax, M. H. Freilich, and R. F. Milliff (2004), Satellite measurements reveal persistent small-scale features in ocean winds, *Science*, 303, 978-983, doi:10.1126/science.1091901.

Cornillion, P. and K. A. Park (2001), Warm core ring velocities inferred from NSCAT, *Geophys. Res. Lett.*, 28, 575-578, doi:10.1029/2000GL011487.

Draper, D. W. and D. G. Long (2004), Evaluating the effect of rain on SeaWinds scatterometer measurements, *J. Geophys. Res.*, 109, C02005, doi:10.1029/2002JC001741.

Ebuchi, N., H. C. Graber, and M. J. Caruso (2002), Evaluation of wind vectors observed by QuikSCAT/SeaWinds using ocean buoy data, *J. Atmos. Oceanic Technol*., 19, 2049-2062.

Freilich, M. H. and Dunbar, R. S. (1999), The accuracy of the NSCAT 1 vector winds: Comparisons with National Data Buoy Center buoys, *Journal of Geophysical Research*, *104*(C5), 11231-11246, doi:10.1029/1998JC900091.

Huddleston, J. N. and M. W. Spencer (2001), SeaWinds: The QuikSCAT wind scatterometer, *Aerospace Conference, IEEE Proceedings*., 4, 1825-1831.

Kara, A. B., A. J. Wallcraft, and M. A. Bourassa (2008), Air-sea stability effects on the 10 m winds over the global ocean: Evaluations of air-sea flux algorithms, *J. Geophys. Res.*, 113, C04009, doi:10.1029/2007JC004324.

Kelly, K. A., S. Dickinson, M. J. McPhaden, and G. C. Johnson (2001), Ocean currents evident in satellite wind data, *Geophys. Res. Lett.*, 28, 2469-2472, doi:10.1029/2000GL012610.

Kent, E. C., P. G. Challenor, and P. K. Taylor (1999), A statistical determination of the random observational errors present in voluntary observing ships meteorological reports, *J. Atmos. Oceanic Technol.,* 14, 905-914.

—, E. C., P. K. Taylor, and P. G. Challenor (1998), A comparison of ship and scatterometer-derived wind speed data in open ocean and coastal areas, *Int. J. of Remote Sens.,* 19, 3361-3381.

Liu, W. T. (2002), Progress in scatterometer application. *J. Oceanogr.,* 58, 121-136.

—, W. T. and X. Xie (2006), Measuring ocean surface wind from space, *Remote Sensing of the Marine Environment, Manual of Remote Sensing, Third Edition, Vol. 6*, J. Gower, Ed., Amer. Soc. For Photogrammetry and Remote Sens., 149-178.

Long, D. G. (2002), High Resolution Wind Retrieval from SeaWinds, *Proc. of the International Geoscience and Remote Sensing Symposium*, **2**, 751-753, doi: 10.1109/IGARSS.2002.1025662.

Portabella, M. and A. Stoffelen (2009), On Scatterometer Ocean Stress, *J. Atmos. Oceanic Technol*., 26, 368-382.

Ross, D.B., V.J. Cardone, J. Overland, R. D. McPherson, W. J. Pierson Jr., and T. Yu (1985), Oceanic surface winds, *Adv. Geophys*., 27, 101–138.

Smith, S. R., J. Rettig, J. Rolph, J. Hu, E. C. Kent, E. Schulz, R. Verein, S. Rutz, and C. Paver (2010), The Data Management System for the Shipboard Automated Meteorological and Oceanographic System (SAMOS) Initiative, *Proceedings of the "OceanObs'09: Sustained Ocean Observations and Information for Society" Conference (Vol. 2)*, Venice, Italy, 21-25 September 2009, Hall, J., Harrison D.E. and Stammer, D., Eds., ESA Publication WPP-306. (in press)

—, S. R., M. A. Bourassa, and R. J. Sharp (1999), Establishing more truth in true winds, *J. Atmos. Oceanic Technol.*, 16, 939-952.

Spencer, M.W., C. Wu, and D.G. Long (2000), Improved resolution backscatter measurements with the SeaWinds pencil-beam scatterometer, *IEEE Transactions on Geoscience and Remote Sensing,* 38, 89-104.

Stoffelen, A. (1998), Toward the true near-surface wind speed: Error modeling and calibration using triple collocation, *Journal of Geophysical Research - Oceans*, *103*(C4), 7755-7766, doi:10.1029/97JC03180.

Taylor, G. I. (1938), The spectrum of turbulence, *Proc. R. Soc.*, 67, 16-20.

Weissman, D. E., K. L. Davidson, R. A. Brown, C. A. Friehe, and F. Li (1994), The relationship between the microwave radar cross section and both wind speed and stress: Model function studies using Frontal Air-Sea Interaction Experiment data, *J. Geophys. Res.,* 99, 10087-10108, doi:10.1029/93JC03371.

—, D. E., M. A. Bourassa, and J. Tongue (2002), Effects of Rain Rate and Wind Magnitude on SeaWinds Scatterometer Wind Speed Errors, *J. Atmos. Oceanic Technol*., 19, 738-746.

BIOGRAPHICAL SKETCH

Jackie Crystal May was born on July 3, 1987 in Pasco, Washington. She grew up in Long Beach, Mississippi, where her family moved to in 1990. Jackie's interest in meteorology began when her dad bought a catamaran while she was in high school: knowing when the best time to sail was largely dependent on the weather. She attended the University of South Alabama and graduated in May 2009 with a Bachelor of Science, double majoring in Meteorology and Mathematics. In August 2009, Jackie came to Florida State University, where she worked as a Graduate Research Assistant for Dr. Mark Bourassa.